Acta Pharmaceutica Sinica B 2023;13(3):942–954

Chinese Pharmaceutical Association
Institute of Materia Medica, Chinese Academy of Medical Sciences

Acta Pharmaceutica Sinica B

www.elsevier.com/locate/apsb
www.sciencedirect.com

ORIGINAL ARTICLE

Sodium alginate coating simultaneously increases the biosafety and immunotherapeutic activity of the cationic mRNA nanovaccine

Xing Duan[a,†], Yi Zhang[b,†], Mengran Guo[b], Na Fan[a], Kepan Chen[a], Shugang Qin[a], Wen Xiao[a], Qian Zheng[a], Hai Huang[a], Xiawei Wei[a], Yuquan Wei[a], Xiangrong Song[a,*]

[a]*Department of Critical Care Medicine, Department of Clinical Pharmacy, Frontiers Science Center for Disease-related Molecular Network, State Key Laboratory of Biotherapy and Cancer Center, West China Hospital, Sichuan University, Chengdu 610041, China*
[b]*West China Hospital, Sichuan University, Chengdu 610041, China*

Received 6 June 2022; received in revised form 10 August 2022; accepted 16 August 2022

KEY WORDS

Negatively charged mRNA vaccine;
Sodium alginate;
Cationic liposome;
DOTAP;
Lysosomes escape;
Cancer;
Immunotherapy;
Toxicity

Abstract The extraordinary advantages associated with mRNA vaccines, including their high efficiency, relatively low severity of side effects, and ease of manufacture, have enabled them to be a promising immunotherapy approach against various infectious diseases and cancers. Nevertheless, most mRNA delivery carriers have many disadvantages, such as high toxicity, poor biocompatibility, and low efficiency *in vivo*, which have hindered the widespread use of mRNA vaccines. To further characterize and solve these problems and develop a new type of safe and efficient mRNA delivery carrier, a negatively charged SA@DOTAP-mRNA nanovaccine was prepared in this study by coating DOTAP-mRNA with the natural anionic polymer sodium alginate (SA). Intriguingly, the transfection efficiency of SA@DOTAP-mRNA was significantly higher than that of DOTAP-mRNA, which was not due to the increase in cellular uptake but was associated with changes in the endocytosis pathway and the strong lysosome escape ability of SA@DOTAP-mRNA. In addition, we found that SA significantly increased the expression of LUC-mRNA in mice and achieved certain spleen targeting. Finally, we confirmed that SA@DOTAP-mRNA had a stronger antigen-presenting ability in E. G7-OVA tumor-bearing mice, dramatically inducing the

*Corresponding author. Tel./fax: +028 8550 3817.
E-mail address: songxr@scu.edu.cn (Xiangrong Song).
[†]These authors made equal contributions to this work.
Peer review under the responsibility of Chinese Pharmaceutical Association and Institute of Materia Medica, Chinese Academy of Medical Sciences

https://doi.org/10.1016/j.apsb.2022.08.015

proliferation of OVA-specific CLTs and ameliorating the antitumor effect. Therefore, we firmly believe that the coating strategy applied to cationic liposome/mRNA complexes is of potential research value in the field of mRNA delivery and has promising clinical application prospects.

1. Introduction

mRNA vaccines have become a promising immunotherapy platform against infectious diseases and cancers on account of their efficacious, scalable, and simple manufacturing process[1−5]. Currently, two mRNA-based SARS-CoV-2 vaccines, BNT162b2 (from Pfizer BioNTech)[6,7] and mRNA-1273 (from Moderna)[8,9], have received FDA marketing approval and emergency use authorization for controlling the SARS-CoV-2 pandemic, respectively, which tremendously accelerated the development of mRNA delivery. The key to the success of mRNA vaccine strategies is to ensure the stabilization of mRNA under physiological conditions and efficient delivery to the target tissue[10]. Consequently, the mRNA delivery vector plays an essential role in stabilizing the mRNA structure, controlling the accessibility to ribosomes and influencing the translational mechanisms[11].

Cationic lipids typically feature a positively charged head group followed by hydrophobic tails of varying composition, which has been widely applied to deliver gene drugs, including DNA, siRNA, and plasmid delivery[12,13], especially mRNA vaccines[2], expanding the flexibility and availability of nucleic acid drugs. Unfortunately, studies have shown that cationic liposomes cause acute cell necrosis in a positive charge-dependent manner[14], and highly positively charged cationic nanovaccines may destroy blood cells and lead to hemolysis[15,16], and Cationic nanocarriers induce acute cell necrosis through the interaction with Na^+/K^+-ATPase, with the subsequent exposure of mitochondrial damage-associated molecular patterns as a key event that mediates the inflammatory responses[17]. Meanwhile, serum proteins could be absorbed by cationic liposomes, form precipitates and are subsequently cleared by the reticuloendothelial system[18,19]. In addition, most liposome/mRNA complexes are trapped in endosomes and lysosomes after endocytosis, where a large number of enzymes affect the stability of the mRNA, resulting in low transfection efficiency[20]. Furthermore, the high positive charge of the liposome/mRNA complex is detrimental to transport to immune organs[10,21], resulting in insufficient uptake of mRNA by immune cells and difficulty in exerting the function of mRNA.

This is based on the important role of mRNA carrier charge and the disadvantages of the highly positive charge of the carrier in regulating mRNA function and the host immune response. Novel carriers and auxiliary phospholipids as well as excipients have been developed to reduce the surface charge of mRNA nanovaccines[22,23]. However, successfully delivering mRNA remains a challenge. Therefore, in this study, from a new perspective, we combined commercial natural anionic pharmaceutical excipients with existing cationic carriers by coating and explored a universal design strategy for mRNA delivery that was simple in prescription, easy to manufacture and clinically transform.

(2,3-Dioleylpropyl)-trimethyl ammonium chloride (DOTAP) is the most representative mRNA delivery carrier due to its extensive research base, relatively low cost, ease of synthesis, and common drawbacks of cationic carriers. More importantly, the study showed that DOTAP has an acceptable safety profile in phase I clinical trials, indicating that DOTAP has promising clinical application prospects[24−28]. On the flip side, the advantages associated with sodium alginate (SA), a widely used and readily available pharmaceutical excipient, including its stability, high solubility, high viscosity, safety and easy production, have enabled it to be an excellent coating material[29−31]. In particular, studies indicate that SA may promote the escape of nanoparticles from lysosomes[32]. Thus, we utilized SA to encapsulate DOTAP liposome/mRNA complexes to prepare a negatively charged nanovaccine and explored its delivery efficiency *in vivo* and *in vitro*, providing a potential and universal design platform for the development of cationic mRNA vaccines with high efficiency and low toxicity. Likewise, our findings provide a simple and feasible method for accelerating the translation of cationic mRNA vaccines in the clinic, and may save some cationic carriers that have failed in clinical practice and help the marketization of old ingredients.

2. Materials and methods

2.1. Materials and reagents

Sodium alginate (SA) and 2-mercaptoethanol were purchased from Runze Local Reagents Co. (Chengdu, China). (2,3-Dioleacyl propyl)-trimethylammonium chloride (DOTAP) and cholesterol (CHOL) were purchased from Avanti Polar Lipids Inc. (Alabaster, USA). mRNA markers were acquired from Ambion (TX, USA). Low melting point agarose was purchased from Thermo Fisher (MA, USA). Bovine serum albumin (BSA) and erythrocyte lytic products were purchased from Sigma−Aldrich (Shanghai, china). GM-CSF was obtained from Peprotech (NJ, USA). APC-anti-mouse CD11C, PE-anti-mouse CD11C, PE-anti-mouse CD80, FITC-anti-mouse CD86, and APC-anti-mouse SIINFEKL/H-2Kb 25-D1.16 were purchased from Biolegend (CA, USA). FITC-conjugated anti-mouse CD3, APC-conjugated anti-mouse CD8a and PE-conjugated anti-mouse CD4 antibodies were purchased from Becton Dickinson and Company (NJ, USA). PE-H-2Kb SIINFEKL tetramer (OVA-tetramer) was obtained from Guangzhou Haozi Biotechnology Co., Ltd. (Guangzhou, China). DMEM, RPMI-1640 medium, fetal bovine serum (FBS), and phosphate buffer (PBS) were purchased from Gibco (New York, USA). Cryogenic refrigerated centrifuges (Thermo Scientific); BX-53 Upright fluorescence microscope (Olympus Corporation, Japan). GFP-mRNA, Luc-mRNA, and OVA-mRNA were constructed and synthesized by other physicians in our laboratory. All other reagents and chemicals were analytical grade.

2.2. Cell line

E. G7-OVA (T lymphoma cell) and DC2.4 (a murine bone marrow-derived dendritic cell line) were purchased from ATCC (American Type Culture Collection). The cells in Dulbecco's modified Eagle's medium (DMEM) containing 10% FBS, 0.1 mg/mL penicillin and 0.1 mg/mL streptomycin were cultured at 37 °C in a 5% CO_2 cell incubator. When the cell density reached 75%−85%, 0.25% trypsin was used for digestion and subculture.

2.3. Experimental animals

Seven-week-old male C57BL/6 mice (body weight ~18 g) were purchased from HFKBio-technology (Beijing, China) and maintained in a specific pathogen-free (SPF) grade animal room in our laboratory; every 6 mice were divided into 1 cage. Mat, food and water were replaced every 3 days. Adaptive feeding was carried out for 1 week before the experiment. All experimental procedures were executed according to the protocols approved by Sichuan University Animal Care and Use Committee.

2.4. Preparation of liposomes/complexes

The empty DOTAP liposomes and empty DOTAP/CHOL liposomes were prepared by the thin-film hydration method. First, 630 μL DOTAP (10 mg/mL) or 630 μL DOTAP and 350 μL (10 mg/mL) cholesterol were added to a round bottom flask, and the lipid membranes were prepared by drying the solvent at 37 °C under vacuum conditions. Then, 3 mL RNase-free ultrapure water was added, and the lipid membranes were collected at 60 °C. After that, the lipid membranes were sonicated for 3 min at 100 W in an ice bath to obtain empty DOTAP liposomes and empty DOTAP/CHOL liposomes. The liposome/mRNA complexes were obtained by incubating the mixture with different mole ratios of *N*/*P* (*N* in DOTAP and *P* in mRNA) of mRNA solution and liposomes at 37 °C for 5 min. SA@DOTAP-mRNA and SA@DOTAP/CHOL-mRNA were prepared by adding the appropriate SA solution to the liposome-mRNA complex and incubating for 5 min.

2.5. Liposome characterization

The zeta potential and average size of these liposome/mRNA complexes were measured by using a Malvern Laser Particle Size Analyzer (Zetasizer Nano ZS 90, Malvern, UK). Data were obtained as an average of more than 3 measurements on different samples.

2.6. Gel retardation assay

The mRNA-binding ability of different liposome/mRNA complexes was evaluated by a gel retardation assay. A total of 0.5 μg of mRNA was separately mixed at different *N*/*P* mole ratios (*N* in DOTAP and *P* in mRNA). The gel was run at a constant voltage of 130 V for 20 min at room temperature. When the leading edge of the indicator reached 2/3 of the gel, the electrophoresis was stopped, and the gel was observed in a gel documentation system (Gel Doc 2000, Bio-Rad Laboratories, Hercules, USA).

2.7. Transfection assay

DC2.4 cells were inoculated in 24-well culture plates (1×10^4 cells/well) supplied with 0.5 mL DMEM (containing 10% FBS) overnight. Briefly, after replacing the medium with different concentrations of FBS, liposome/mRNA complexes containing 1 μg GFP-mRNA were added to each well for incubation for 24 h. Finally, inverted fluorescence microscopy (Nikon, Japan) and flow cytometry (FACS, BD AccuriC6, USA) were used to evaluate the transfection effect.

2.8. Study of cellular uptake

DC2.4 cells were seeded on 24-well culture plates (1×10^5 cells/well) and incubated overnight in 0.5 mL DMEM containing 10% FBS. The medium was replaced with fresh DMEM containing 10% FBS, and liposome/mRNA complexes containing 1 μg CY5-mRNA were added to each well. The cells were collected 6 h later and washed twice with PBS, and flow cytometry was used to evaluate the fluorescence intensity of each well. Besides, spleen single cells of mice were seeded on 24-well culture plates (1×10^6 cells/well) and incubated 30 min in 0.5 mL DMEM containing 10% FBS, and DOTAP/CHOL-CY5, DOTAP-CY5 and SA@DOTAP-CY5 were added to each well, the cells were collected 6 h later and washed twice with PBS. Finally, flow cytometry was used to evaluate the fluorescence intensity of each well.

2.9. Cellular uptake pathway

DC2.4 cells were seeded on 24-well culture plates (1×10^5 cells/well) and incubated overnight in 0.5 mL DMEM containing 10% FBS. Then, the medium was replaced by 500 μL DMEM with different uptake inhibitors. (Dosage of ingestion inhibitor: Chlorpromazine, 5 μg/well; cytochalasin D, 0.255 μg/well; nystatin, 5 μg/well). After 0.5 h of incubation, liposome/mRNA complexes containing 1 μg CY5-mRNA were added to each well for incubation for 2 h. Finally, the cells were collected, and the fluorescence intensity was evaluated by flow cytometry.

2.10. Lysosome escape

DC2.4 cells were inoculated in confocal dishes (1×10^5 cells/well) supplied with 2 mL DMEM (containing 10% FBS) overnight. CY5-mRNA was used as a tracer, and LysoTracker was used as a lysosome marker. Liposome/mRNA complexes loaded with CY5-mRNA (the final concentration of CY5-mRNA was 0.5 μg/plate) were added to each plate and incubated at 37 °C for 2 h in the dark. After reaching the incubation time point, the medium was discarded, and the cells were washed twice with precooled PBS to remove the nanovaccines adsorbed on the cell surface [1 h before the termination of uptake, lysosome marker (75 μmol/L final concentration Lyso-Tracker) was added to mark the lysosome]. The cells were precooled and rinsed twice with PBS. Confocal microscopy was used for observation and photography.

2.11. Detachment activity of SA@DOTAP-mRNA

The pH of SA@DOTAP-mRNA were adjusted with dilute hydrochloric acid, and then stand for 30 min and the average size of these SA@DOTAP-mRNA were measured by using a Malvern Laser Particle Size Analyzer (Zetasizer Nano ZS 90, Malvern,

UK). Data were obtained as an average of more than three measurements on different samples.

2.12. Preparation of bone marrow-derived dendritic cells (BMDCs)

BMDCs were generated as previously described. Briefly, bone marrow cells from the tibia and femur of C57 mice were rinsed with a syringe and then treated with precooled red blood cell solution for 5 min, and the cells were collected by centrifugation. The cells were cultured in BMDC medium (1% penicillin streptomycin, 0/1% 2-mercaptoethanol, 10% FBS, 89% RPMI-1640 medium and 0.2 μg GM-CSF) at 37 °C in a 5% CO_2 cell incubator for 3 days. Then, 10 mL of BMDC medium was added to the Petri dish and cultured until Day 7 to obtain immature BMDCs.

2.13. BMDCs maturation and antigen presentation

BMDCs were inoculated in 24-well culture plates (5×10^5 cells/well) supplied with 0.5 mL RPMI-1640 medium (containing 10% FBS) for 0.5 h, and then liposome/mRNA complexes containing 1 μg OVA-mRNA were added to each well for incubation for 24 h. Then, BMDCs were harvested and labeled with PE-anti-mouse CD11c, FITC-anti-mouse CD86, and APC-anti-mouse SIINFEKL/H-2Kb 25-D1.16. Flow cytometry (NovoCyteTM, Eisen Bioscience, USA) was used to detect the antigen presentation of BMDCs.

2.14. In vivo distribution of liposome complexes

In vivo distribution and expression of DOTAP-mRNA, DOTAP/CHOL-mRNA, and SA@DOTAP-mRNA was detected in male C57BL/6/C mice aged 6−7 weeks, with 3 mice in each group. CY5-mRNA and LUC-mRNA was used as a tool mRNA, and the dosage of mRNA was 30 μg/mouse. The mice were euthanized 6 h after injection, and the heart, liver, spleen, lung and kidney were separated to investigate the distribution and expression of different liposome/mRNA complex delivery systems *in vivo* by *ex vivo* imaging.

2.15. Immunization of mice and tumor inoculation

During the logarithmic growth phase of E. G7 cells, the cells were collected and washed with sterile PBS, and the cell density was adjusted to 5×10^6 cells/mL. Each mouse was subcutaneously inoculated with 100 μL E. G7 cells on the right side of the ribs. Tumor formation was observed 5 days after inoculation, and immunotherapy was administered on Day 7. Body weight and tumor volume were measured every 2 days and immunized every 5 days.

2.16. OVA-specific T-cell testing

After 3 immunizations, normal mice and E. G 7-OVA-bearing mice, spleen and tumor single cells of mice were collected in flow tubes. First, the cells were treated with erythrocyte lysate for 10 min and then washed twice with PBS. Then, 1 μL FITC-anti-mouse CD3, 1 μL APC-anti-mouse CD8A and 1 μL H-2kB OVA tetramer SIINFKL/H-2Kb were added to the flow tubes and incubated in the dark at 4 °C for 40 min. Finally, OVA-specific T cells were detected by flow cytometry.

2.17. Cytotoxicity assay

CCK8 was used to detect the cytotoxicity of liposome/mRNA complexes to DC2.4 cells. Briefly, DC2.4 cells were seeded onto 96-well plates (the cell density was 1×10^4 cells/well), and 24 h later, different amounts of nano vaccine were added to each well. After 24 h of incubation, 10 μL of CCK8 was added to each well, the cells were incubated at 37 °C for 4 h, and the cell viability was measured by using a microplate reader assay following the manufacturer's protocol.

2.18. Hemolysis test

Take 10 mL of fresh rat blood and put it in a beaker with 100 mL normal saline, or stir the blood with a glass rod to remove the fiber protein and make defibrillated blood. Then centrifuge the supernatant with 1000−1500 rpm for 15 min to remove the red blood cells, and then wash the precipitated red blood cells with normal saline for 2−3 times according to the above method until the supernatant does not show red color. The red blood cells were prepared with normal saline into 2% suspension for experimental use. The samples were successively added into 2% red blood cell suspension, and immediately placed in a thermostatic water bath at 37 °C for incubation for 2 h. Finally, the hemolysis rate of the preparation was detected by a microplate meter.

2.19. Blood biochemical index detection

After the administration of different liposome/mRNA complexes for 24 h, the serum was obtained by centrifugation, and the contents of alanine aminotransferase (ALT), aspartic acid aminotransferase (AST), total protein (TP), uric acid (UA) and urinary anhydride (URREAL) in all plasma samples were determined by using serological biochemical analysis with an automatic analyzer (Hitachi High-Technologies Corp., Minato-ku, Tokyo, Japan).

2.20. Histopathological evaluation

After treatment, one mouse in each group was randomly selected, its vital organs were collected, and pathological tissue sections of each organ were prepared and stained. The stained tissues were observed and photographed in a pathological section scanner, and the pathological changes in the liver, kidney, spleen, lung and other important tissues and organs of mice were investigated.

2.21. Statistical analysis

0rigin 2019 software was used to prepare all graphs and perform statistical analysis, including one-way ANOVA. All experiments were performed in triplicate unless otherwise stated. Error bars indicate standard deviation (SD). $P < 0.05$ value is considered statistically significant, and all statistically significant values shown in figures are indicated as: $^{*}P < 0.05$ and $^{***}P < 0.001$.

3. Results and discussion

3.1. Optimization and characterization of the liposome/mRNA complex

mRNA vaccines are hailing a new era in vaccinology[1]. mRNA is very easy to obtain, but the development of mRNA vectors that are used for the efficient and safe delivery of mRNA is relatively

sluggish, making it difficult to achieve clinical translation of most of the mRNA that has been proven to be effective, which has negatively restricted the progress of mRNA vaccines[33]. Therefore, the research and development of new carriers have always been a hot topic in the mRNA delivery field. However, in some cases, they may be difficult to synthesize and much more expensive than existing cationic lipids. Furthermore, the available clinical data of novel carriers are inadequate from a regulatory and safety perspective[34]. The use of existing carriers to achieve efficient and safe delivery of mRNA has always been the focus of our thinking. Therefore, in this work, a negatively charged nanovaccine was prepared by coating cationic liposome/mRNA complexes with SA to solve the defects of traditional cationic mRNA vaccines and explore a new method of gene delivery.

To obtain the liposome/mRNA complexes, agarose gel electrophoresis was first applied to detect the binding ability of mRNA and DOTAP liposomes. The results showed that mRNA was completely wrapped by DOTAP liposomes when the molar ratio of N/P (N in DOTAP and P in mRNA) was 3:1 or above (Supporting Information Fig. S1). As the liposome/mRNA complex is positively charged, SA could wrap around the mRNA liposome *via* electrostatic interactions. At present, the particle size of SA/DOTAP/CHOL-mRNA increases geometrically, the zeta potential decreases continuously, and the PDI increases significantly with increasing mass ratio of sodium alginate to mRNA. Stable and uniform SA@DOTAP/CHOL-mRNA could not be formed (Fig. 1A). We hypothesize that the stabilizing effect of CHOL on lipid membranes limits the interaction between cationic lipid DOTAP and anionic polymer SA, making it difficult to form stable nanovaccines. To test this hypothesis, we used an SA-coated DOTAP-mRNA nanovaccine without CHOL for experimental verification. As expected, we found that SA@DOTAP-mRNA had moderate and uniform particle sizes. Meanwhile, the zeta potential decreased continuously with increasing SA and finally became negative, indicating that DOTAP-mRNA was successfully coated by SA (Fig. 1B). Furthermore, by investigating the structure of the mRNA nanovaccine and the particle size distributions of SA@DOTAP/CHOL-mRNA and SA@DOTAP-mRNA at the same SA-to-mRNA mass ratio (Supporting Information Figs. S2 and S3), we confirmed that CHOL was not conducive to liposome/mRNA encapsulation by SA.

More importantly, as we speculated, the interaction between DOTAP and SA was limited by CHOL. SA substantially increased the transfection efficiency of DOTAP-GFP and markedly decreased the transfection efficiency of DOTAP/CHOL-GFP both in the presence and absence of serum (Fig. 1C–H). To the best of our knowledge, this is the first study to indicate that the presence of CHOL was not conducive to the coating of liposome/mRNA complexes, which may be the reason why such a coating strategy has rarely been used for liposome/mRNA complex delivery in previous studies. Our work may provide the initial framework for future research and development of liposome mRNA nanovaccines based on the coating method.

3.2. *Transfection assay and stability*

Since SA@DOTAP-GFP had the optimal transfection effect when the mass ratio of mRNA to SA was 1:1, we selected SA@DOTAP-GFP when the mass ratio of mRNA to SA was 1:1 for subsequent studies. To accurately evaluate the effect of SA@DOTAP-mRNA, DOTAP/CHOL-GFP was prepared by classical prescription as the positive control. GFP transfection experiments were performed in DC 2.4 cells. We found that SA not only dramatically enhanced the transfection of DOTAP-GFP, but its transfection efficiency was also significantly higher than that of DOTAP/CHOL-GFP (Fig. 2A–D).

Generally, SA@DOTAP-mRNA has a simpler prescribing composition than LNPs now used in clinic. The readily available raw materials, oversimplified prescription and process provide the feasibility of the industrial production of SA@DOTAP-mRNA. To further investigate the clinical transformation prospects of SA@DOTAP-mRNA, we investigated its storage stability. The liposome complex was stored at 4 °C, and the stability of these liposome/mRNA complexes was tested by particle size, PDI, and zeta potential. We found that SA@DOTAP-GFP had a more homogeneous property than DOTAP-GFP and DOTAP/CHOL-GFP, its PDI was smaller, and its particle size, zeta potential and PDI did not vary significantly during preservation. These results showed that SA stabilized cationic liposomes (Fig. 2E–G). In addition, through gel electrophoresis experiments, we did not find mRNA leakage from DOTAP-GFP, SA@DOTAP-GFP, and DOTAP/CHOL-GFP, indicating that SA has no impact on the loading capacity of cationic liposomes on mRNA (Fig. 2H). More importantly, we found that SA@DOTAP-GFP had better transfection stability than DOTAP-GFP and DOTAP/CHOL-GFP (Fig. 2I and J). We speculate that the loading of mRNA by cationic liposomes blocks the degradation of mRNA by RNase. However, some mRNA that are loosely wrapped by cationic liposome could still be degraded by RNase, and SA's modification further blocks RNase's degradation of those mRNA. Hence, we prepared SA@DOTAP-GFP with GFP mRNA stored at 4 °C for 28 days to repeat the transfection effect of SA@DOTAP-GFP. The transfection efficiency of SA@DOTAP-GFP(d28) was significantly reduced, while that of SA@DOTAP-GFP(d0) remained high, as shown in Supporting Information Fig. S4, which suggests that SA@DOTAP-mRNA has promising prospects for industrial production and clinical application.

3.3. *Transfection mechanism*

To explore whether the higher transfection efficiency of SA@DOTAP-GFP is related to cell uptake, confocal microscopy (Fig. 3A) and flow cytometry (Fig. 3B) were used to investigate the cellular uptake of DOTAP-CY5, DOTAP/CHOL-CY5, and SA@DOTAP-CY5 in DC2.4 cells. The results show that both SA and CHOL upregulated the endocytosis of DOTAP-CY5, but there was no significant difference in the endocytosis of DOTAP/CHOL-CY5 and SA@DOTAP-CY5 (Fig. 3A–C). Since there was no difference in the total cell uptake of SA@DOTAP-GFP and DOTAP/CHOL-GFP, we speculated that the higher transfection efficiency of DOTAP/CHOL-GFP might be related to the mechanism of endocytosis. Therefore, we pretreated cells with cell uptake inhibitors. As expected, the cell uptake amount of DOTAP/CHOL-CY5, DOTAP-CY5 and SA@DOTAP-CY5 was reduced after pretreatment with clathrin and the macropinocytosis inhibitor chlorpromazine and cytochalasin D. Unexpectedly, the cell uptake amount of SA@DOTAP-CY5 was also reduced by the inhibitor nystatin (Fig. 3C), which indicated that SA@DOTAP-mRNA entered cells *via* the caveolin-mediated pathway. Upon reviewing the literature, caveolin-dependent endocytosis has been shown to be a convenient pathway to bypass the fusion of lysosomes[35,36]. The vaccine based on caveolin-dependent endocytosis is eventually delivered to the endoplasmic reticulum (ER), where ribosomes and major histocompatibility complex (MHC)

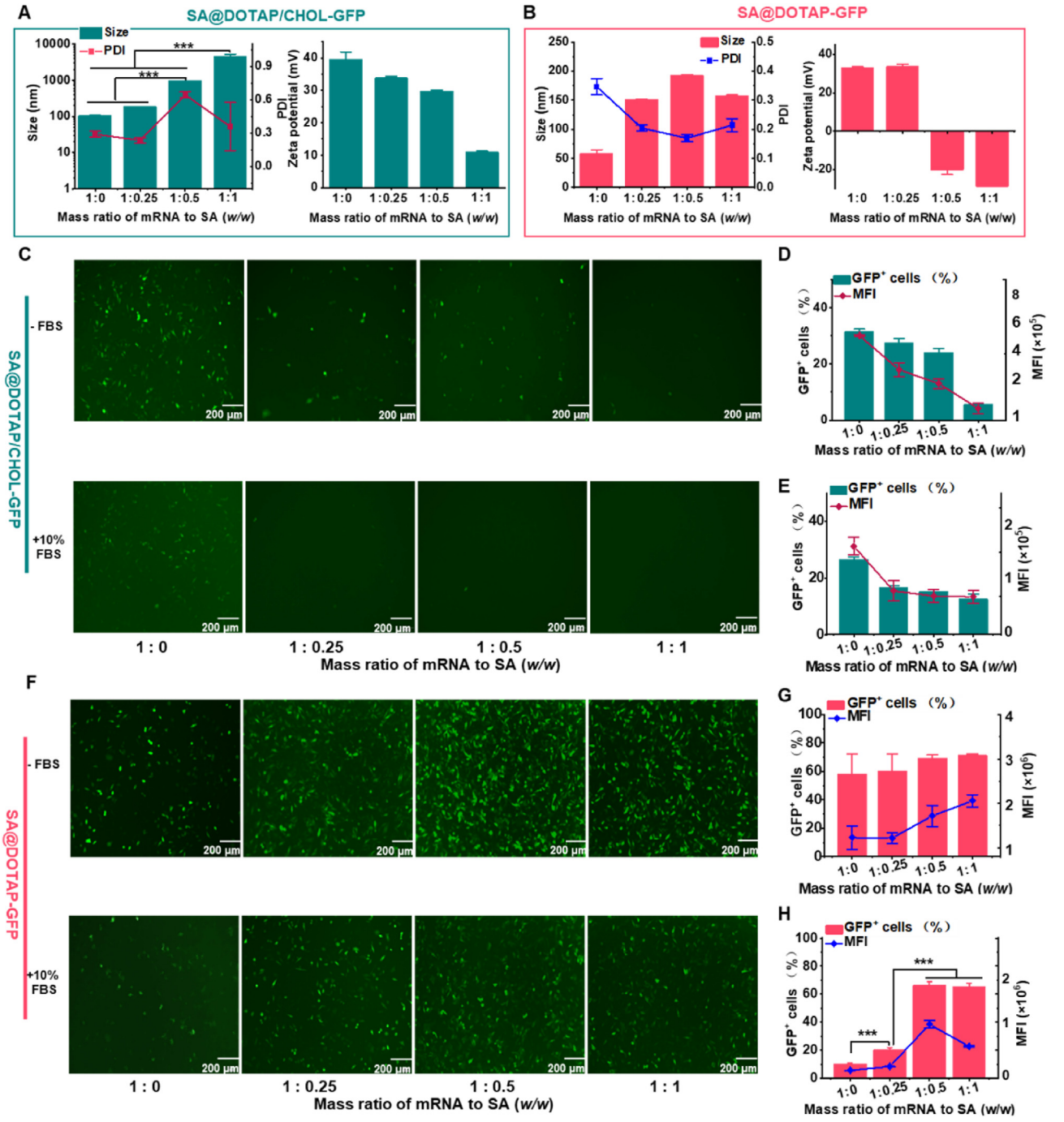

Figure 1 Optimization and characterization of SA-modified liposome/mRNA complexes. (A, B) Particle sizes and ζ-potentials of SA@DOTAP/CHOL-mRNA and SA@DOTAP-mRNA were prepared with different mass ratios of mRNA to SA. (C−H) GFP expression images (left) and quantitative analysis (right) of SA@DOTAP/CHOL-GFP and SA@DOTAP-mRNA in DC 2.4 cells under 10% serum and serum-free conditions. Data are presented as mean ± SD ($n = 3$), ***$P < 0.01$, scale bar = 200 μm.

molecules in the ER provide a convenient pathway for mRNA translation and antigen presentation[37]. This may account for the efficient translation and antigen presentation of SA@DOTAP-mRNA (Fig. 2A).

The internalized liposome/RNA complex must evade endosome or lysosome function[38]. Therefore, the lysosome escape ability of DOTAP-CY5, SA@DOTAP-CY5, and DOTAP/CHOL-CY5 was investigated by confocal laser microscopy. The experimental results showed that DOTA-CY5 and DOTAP/CHOL-CY5 colocalized with lysosomes to varying degrees, while SA@DOTAP-CY5 had a low colocalization rate with lysosomes (Fig. 3D). Consistent with previous reports, our data showed that SA has some characteristics of anionic polymers and improves the escape ability of nanodrugs from lysosomes. It is possible that SA side chains are neutralized by H^+ and detached as the pH decreases, followed by the uncharged hydrophobic side chain inserting into the hydrophobic part of the

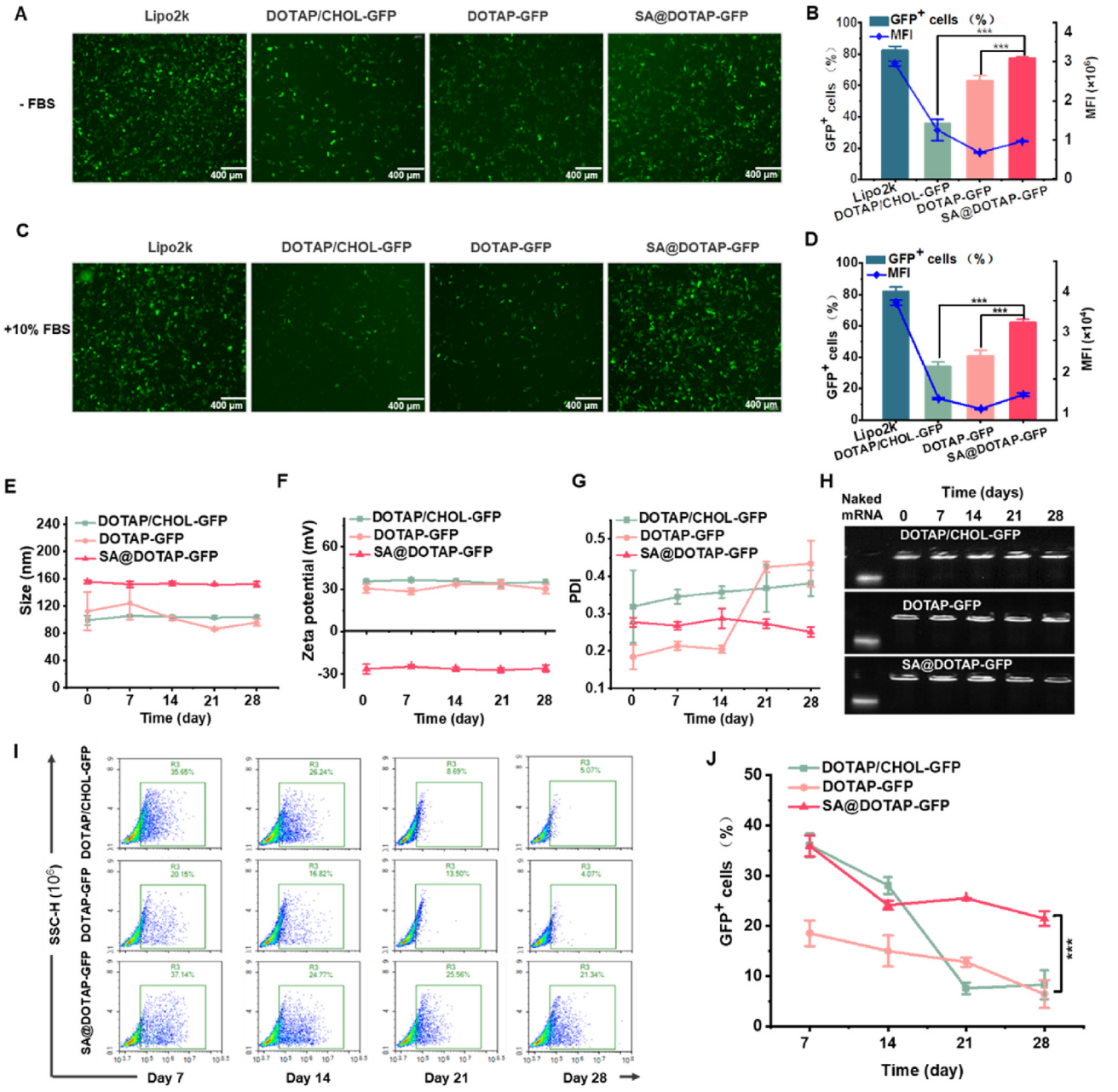

Figure 2 Transfection effect and stability of Lipo2k and DOTAP/CHOL-GFP (positive control) DOTAP-GFP and SA@DOTAP-GFP. (A−D) GFP expression images (left), quantitative analysis (right) of DOTAP/CHOL-GFP DOTAP-GFP and SA@DOTAP-mRNA in DC 2.4 cells under 10% serum and serum-free conditions scale (bar = 200 μm). (E−G) The variation in particle size, potential and PDI of DOTAP/CHOL-GFP, DOTAP-GFP and SA@DOTAP-GFP over time. (H) Gel retardation assay to investigate the mRNA loading stability of DOTAP/CHOL-GFP DOTAP-GFP and SA@DOTAP-GFP. (I, J) FACS analysis to investigate the mRNA transfection stability of DOTAP/CHOL-GFP DOTAP-GFP and SA@DOTAP-GFP. Data are presented as mean ± SD ($n = 3$). ***$P < 0.01$, scale bar = 200 μm.

endosomal membrane, reducing endosomal stability and facilitating endosomal escape[39,40]. On the flip side, cationic lipids break the lysosome membrane by fusing with anionic phospholipids on the lysosome membrane, thus mediating lysosome escape of liposomes[20]. In this study, our prescription only contained mRNA, cationic lipids DOTAP, and the coating material SA. DOTAP-mRNA was exposed after SA binding hydrogen ions and shedding. DOTAP molecules were more easily fused with the lysosomal membrane without the stabilizing effect of CHOL on the lipid membrane of DOTAP-mRNA, thus improving the lysosomal escape effect. At the same time, we simulated the process of SA@DOTAP-mRNA entering lysosome *in vitro* by adjusting PH, and tested its particle size under different PH conditions, so as to detect the analytical attachment activity of SA. The results are shown in Supporting Information Fig. S5, with the decrease of PH, the particle size of SA@DOTAP-mRNA increases gradually, which further

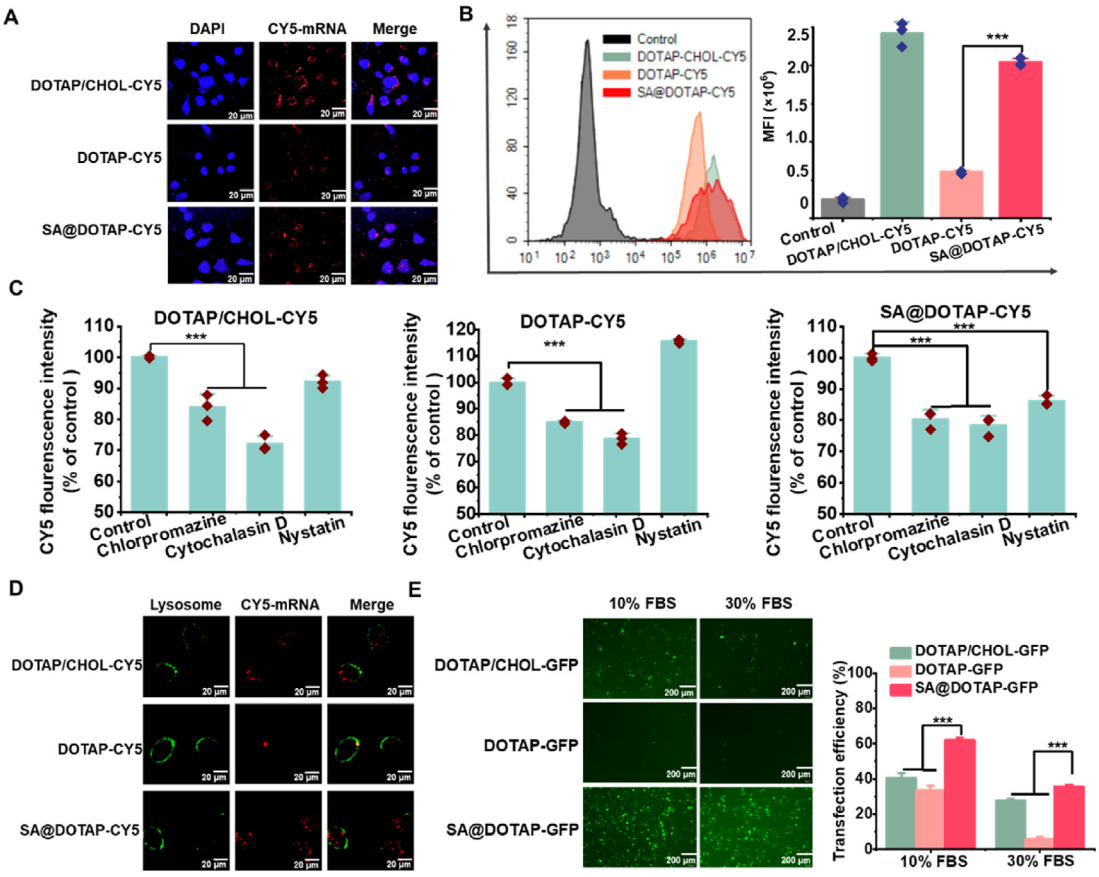

Figure 3 Transfection mechanism study. (A) Laser scanning confocal microscopy (LSCM) images of DC2.4 cells treated with DOTAP/CHOL-CY5, DOTAP-CY5 and SA@DOTAP-CY5 for 5 h (scale bar = 20 μm). (B) FACS analysis of the mean fluorescence intensity of $Cy5^+$ DC 2.4 cells treated with PBS, DOTAP/CHOL-CY5, DOTAP-CY5 and SA@DOTAP-CY5 for 2 h. (C) Cell uptake assay of DOTAP/CHOL-CY5, DOTAP-CY5 and SA@DOTAP-CY5 after treatment with different cell uptake inhibitors. (D) CLSM images show the lysosome escape of DOTAP/CHOL-CY5, DOTAP-CY5 and SA@DOTAP-CY5 in DC2.4 cells (scale bar = 20 μm). (E) Transfection efficiency of DOTAP/CHOL-GFP, DOTAP-GFP and SA@DOTAP-GFP in 10% and 30% FBS. Data are presented as mean ± SD (n = 3, cale bar = 200 μm). ***$P < 0.01$.

proves that SA helps cationic liposomes achieve lysosomal escape by neutralizing H^+.

To verify whether SA@DOTAP-GFP increased transfection by decreasing serum protein adsorption, as we expected. We conducted transfection experiments in DC2.4 cells under the condition of a high concentration of FBS, and the experimental results proved that SA/DOTAP-GFP still maintained high transfection efficiency in 30% FBS, while the transfection efficiency of DOTAP-GFP and DOTAP/CHOL-GFP was significantly reduced (Fig. 3E). In addition, an aqueous solution containing 50% FBS was coincubated with DOTAP-GFP, DOTAP/CHOL, and SA@DOTAP-GFP, and the particle size changes of these three liposome/mRNA complexes were measured. Compared with DOTAP-GFP and DOTAP/CHOL-GFP, the particle size of SA@DOTAP-GFP did not change significantly with incubation time, which means that SA dramatically reduces the adsorption of DOTAP to FBS (Supporting Information Fig. S6). We believe that this may be another reason for the higher transfection efficiency of SA@DOTAP-GFP.

3.4. *Immune activity*

To verify whether SA@DOTAP-mRNA with high transfection also boosts the antigen presentation effect, antigen presentation and activation of BMDCs were investigated after the purity of BMDCs complies with the requirements (Supporting Information Fig. S7). The experimental results showed that SA@DOTAP-OVA had a stronger antigen presentation effect than DOTAP-OVA and DOTAP/CHOL-OVA (Fig. 4A). This may be related to the strong transfection ability of the mRNA nanovaccine coated with sodium alginate on BMDCs (Supporting Information Fig. S8). *In vitro* experiments have confirmed that SA@DOTAP-mRNA has strong transfection ability. Generally, serum protein would be adsorbed by the cationic gene vaccine, resulting in the formation of polymeric precipitates easily cleared by the reticuloendothelial system. Hence, the gene vaccine with a positive charge cannot reach the target organ smoothly[19]. Although it has been reported that adding anionic phospholipids to cationic carriers could reduce the adsorption of vaccines to serum protein by reducing the zeta potential of liposomes[10,23], this strategy not only damages the capacity of liposomes to load mRNA but also greatly limits the stability of the prepared liposomes because the mixing of positive and negative ions is prone to precipitate. Therefore, the strategy of anionic polymer coating may have certain advantages for the delivery of nanopreparation *in vivo*.

In this study, we studied the distribution and expression of DOTAP-mRNA, DOTAP/CHOL-mRNA, and SA@DOTAP-

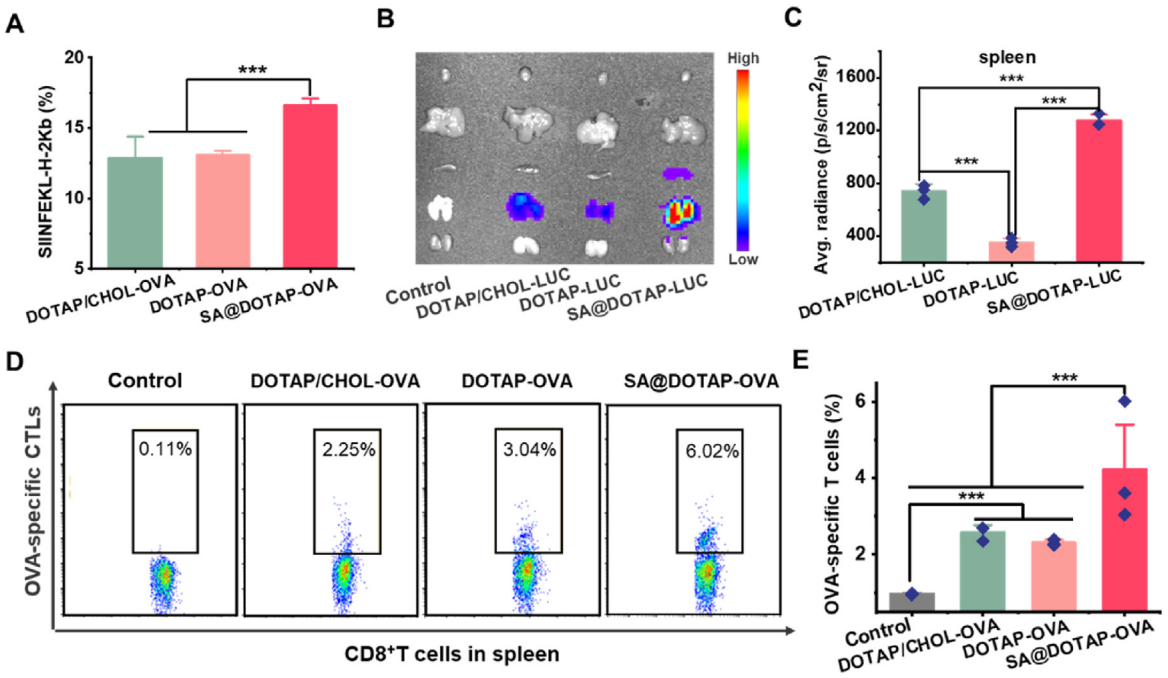

Figure 4 Immune activity of DOTAP/CHOL-mRNA, DOTAP-mRNA and SA@DOTAP-mRNA *in vitro* and *in vivo*. (A) Antigen presentation of DOTAP/CHOL-OVA, DOTAP-OVA and SA@DOTAP-OVA in BMDCs. (B) The *in vivo* expression of luciferase in mice after intravenous injection with DOTAP/CHOL-LUC, DOTAP-LUC and SA@DOTAP-LUC. (C) Quantitative analysis of luciferase expression in the spleens of mice treated by DOTAP/CHOL-LUC, DOTAP-LUC and SA@DOTAP-LUC, respectively. (D, E) FACS analysis of OVA-specific CTL proliferation in the spleen. Data are presented as mean ± SD ($n = 3$). ***$P < 0.01$.

mRNA, and the experimental results showed that the distribution and expression of SA@DOTAP-mRNA in the lungs of mice was significantly higher than that of DOTAP-mRNA and DOTAP/CHOL-mRNA. More importantly, the distribution and expression of SA@DOTAP-mRNA in the spleen was also significantly higher than that of DOTAP-mRNA and DOTAP/CHOL-mRNA, suggesting that changing the electrical properties of liposomes is a feasible way to change the distribution of cationic liposomes (Fig. 4B and C, and Supporting Information Fig. S9). At the same time, we also detected that the uptake efficiency of SA@DOTAP-mRNA by spleen DC cells was higher than that of DOTAP/CHOL-mRNA and DOTAP-mRNA (Supporting Information Fig. S10).

Furthermore, we explored whether the high transfection efficiency and strong antigen presentation ability of SA@DOTAP-OVA could also better promote the proliferation and differentiation of T cells into specific CTLs. After immunizing normal mice 3 times according to the treatment regimen, a cell suspension of spleen cells was prepared. Flow cytometry was used to detect specific CTLs in the spleens of mice. The results showed that DOTAP-OVA and DOTAP/CHOL-OVA had no significant difference in promoting the proliferation of OVA-specific CLTs, while SA@DOTAP-OVA significantly promoted the proliferation of OVA-specific CLTs (Fig. 4D and E). This may be related to the strong antigen presentation ability of SA@DOTAP-OVA on DC cells of the spleen (Supporting Information Fig. S11). In addition, we found that SA@DOTAP-OVA significantly increased lymph node weight in the treated mice (Supporting Information Fig. S12). The high antigen presentation ability promoted the proliferation of OVA-specific CLTs and provided the possibility for an efficient antitumor immune response.

3.5. *In vivo antitumor effects*

TCR activation and IFN signaling could also be dependent on the route of mRNA administration, ultimately impacting CTL activation[35]. Based on this view, some studies suggest that mRNA vaccination *via* intravenous injection could avoid the adverse effects of innate immunity inherent in mRNA and promote $CD8^+$ T-cell responses[41,42]. Hence, in this study, we developed an intravenous vaccine. After confirming the strong immune activity of SA@DOTAP-OVA in mice, we conducted pharmacodynamic experiments. EG7 tumor-bearing mice were treated with different liposome/mRNA complexes injected through the mouse tail vein. Compared with the normal saline group, tumor growth was inhibited by increasing the antigen presentation effect in all groups, while SA@DOTAP-LUC had a slight inhibitory effect on tumor growth, which may be caused by DOTAP itself having a certain immune adjuvant effect. There was no significant difference in therapeutic effect between DOTAP/CHOL-OVA and DOTAP-OVA, while the antitumor effect of SA@DOTAP-OVA was significantly higher than that of DOTAP-OVA. Although we did not detect an obvious difference in tumor volume (Fig. 5G) and weight (Fig. 5H) between the DOTAP/CHOL-OVA group and the SA@DOTAP-OVA group, the tumors in the SA@DOTAP-OVA group showed significant regression after slowly growing up 3−5 days from the tumor growth trend after the last administration. We speculated that the reason why the tumor did not immediately regress after immunization might be that it takes a certain time for the immune effect of the vaccine to take effect. More importantly, we found that tumor-infiltrating OVA-specific CTLs in the SA@DOTAP-OVA group were significantly higher than those in the DOTAP/CHOL-OVA group (Fig. 6H−I and Supporting Information Fig. S13), suggesting that SA@DOTAP-

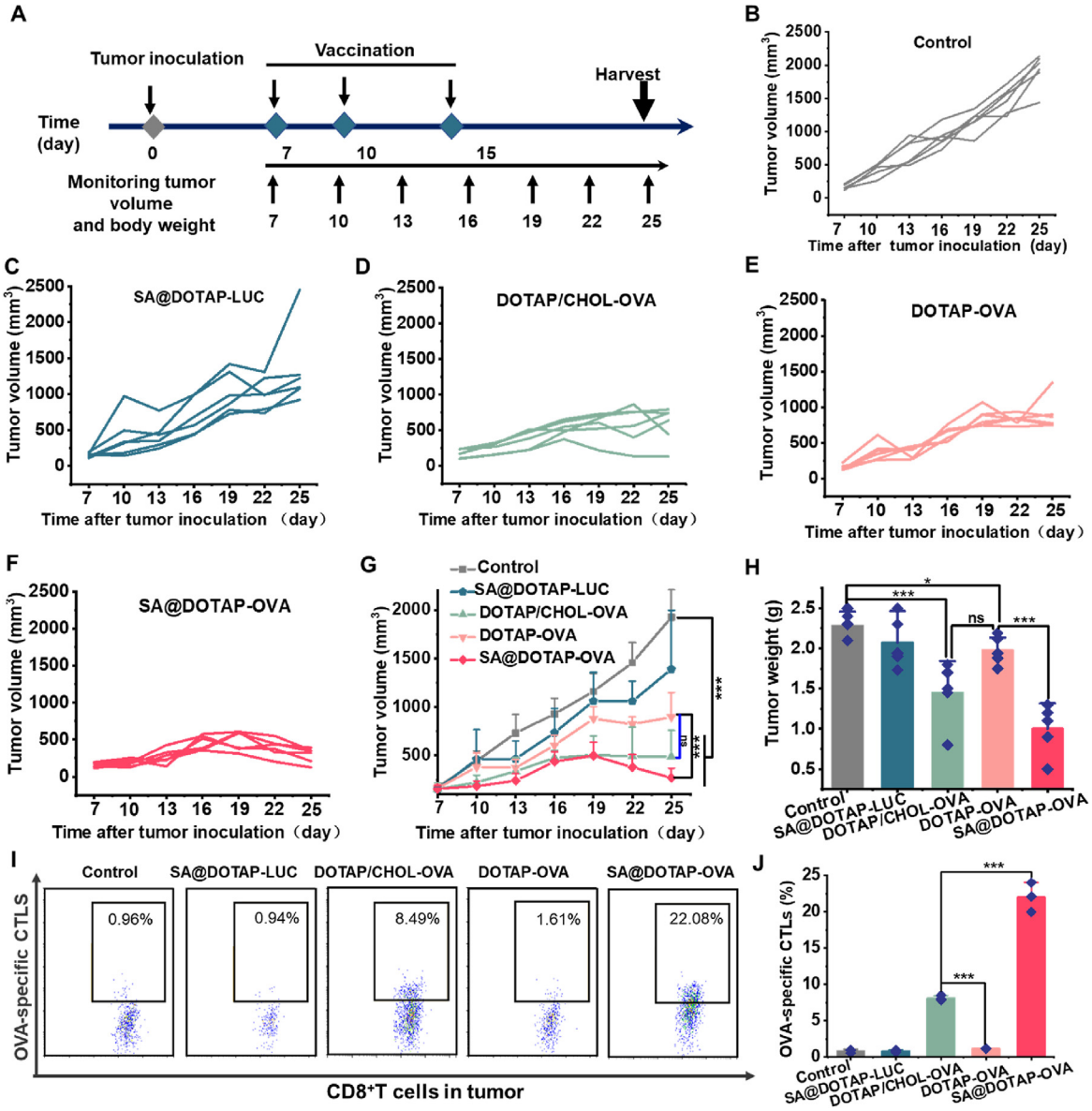

Figure 5 The antitumor activity of DOTAP/CHOL-OVA, DOTAP-OVA and SA@DOTAP-OVA. (A) Schematic diagram of the immunotherapy regimen. (B−F) Tumor growth of each mouse in different groups. (G) Growth of tumor volume in different groups of mice. Data are presented as mean ± SD ($n = 6$). *$P < 0.005$, ***$P < 0.01$. ns, not significant. (H) Tumor weight in different groups of mice after the therapy (mean ± SD, $n = 6$). *$P < 0.05$, ***$P < 0.01$. (I,J) FACS analysis of OVA-specific CTL proliferation in the tumor (mean ± SD, $n = 3$). ***$P < 0.01$.

OVA has a stronger antitumor effect than DOTAP/CHOL-OVA. Further studies will consider optimizing the administration regimen to improve the antitumor activity of SA@DOTAP-OVA.

3.6. *Safety and toxicity evaluations of SA@DOTAP-mRNA*

Considering that the method of injection was used in this study, the toxicities and side effects of the vaccine were the focus of our attention. To test whether SA reduces the toxicity of cationic liposomes, we tested the cytotoxic effect of DOTAP/CHJOL-OVA, DOTAP-OVA, and SA@DOTAP-OVA by CCK8, and the results showed that SA@DOTAP-OVA showed lower toxicity than DOTAP-OVA and DOTAP/CHOL-OVA (Fig. 6A). Besides, through the hemolysis test, we found that the SA@DOTAP-mRNA modified with SA significantly reduced hemolysis, and DOTAP-OVA and DOTAP/CHOL-OVA causes severe hemolysis (Supporting Information Fig. S14), which proved that These results demonstrate that SA modification is a reliable means to improve the safety of cationic nanovaccines.

There were no abnormal changes in body weight during the treatment (Supporting Information Fig. S15). To further study the safety of SA@DOTAP-OVA on the physiology of mice, H&E staining and biochemical analysis were carried out, and the results are shown in Fig. 6B−F. In contrast to the literature reports[14,43], DOTAP/CHOL-OVA did not show obvious pulmonary toxicity in mice by H&E staining (Fig. 6G). We speculate that this may be due to the insufficient current immunization dose to cause organ damage or to the fact that organ tissue damage had already recovered at the time of sampling, since organ tissue was collected 7 days after the last immunization in this study. However, the

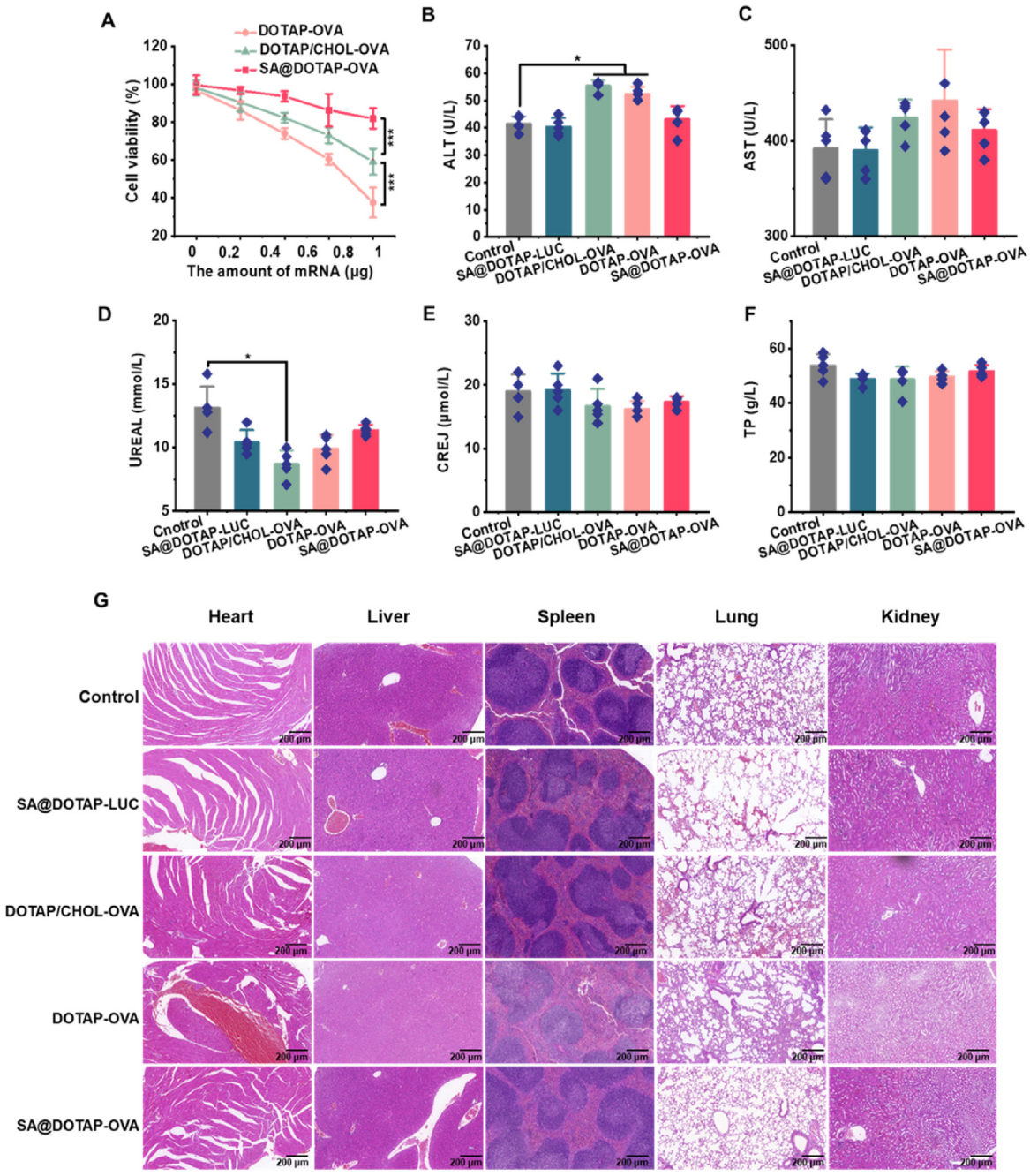

Figure 6 Biocompatibility test of nanoparticles *in vitro* and *in vivo*. (A) Toxicity test of liposome/mRNA complexes in DC2.4 cells. (B,C) Liver function assay of mice with different treatments. (D−F) Renal function assay of mice with different treatments. Data are presented as mean ± SD ($n = 3$). *$P < 0.005$. ***$P < 0.001$. (G) H&E staining of heart, liver, spleen, lung and kidney pathology 10 days after the initial immunization (scale bar = 200 μm).

biochemical indices suggested that DOTAP-OVA and DOTAP/CHOL-OVA caused damage to key organs, such as the liver and kidney, in mice, but SA@DOTAP-OVA did not cause significant organ damage in mice. This evidence suggested that the damage to the functions of DOTAP-OVA- and DOTAP/CHOL-OVA-treated mouse vital organs was reduced by the addition of SA. Overall, SA alleviated the tissue toxicity and inflammation induced by DOTAP-OVA in mice, which suggests that modifying SA establishes a safer formulation of liposome/mRNA complexes for gene therapy. Although the effect of delivery based on the ionizable lipids has been clinically recognized, there are still some patients with adverse reactions[44]. Therefore, it is necessary to continuously explore new delivery systems. In future studies, we will consider more in-depth safety evaluation of SA@DOTAP-mRNAs, hoping

to obtain more comprehensive data to support future clinical studies of anionic mRNA delivery systems.

4. Conclusions

In this work, we have pioneered proof of the concept that negatively charged liposomes can be used as highly efficient mRNA delivery carriers and that this nanovaccine is powerful for tumor immunotherapy in mice. The mRNA-loaded nanovaccine (SA@DOTAP-mRNA) with an oversimplified prescription, high stability, and ease of manufacture was obtained by coating the natural anionic polymer sodium alginate (SA) on cationic liposomes (DOTAP-mRNA) containing DOTAP and mRNA. We found that the negatively charged mRNA vaccine based on the coating strategy has mickle advantages that the traditional positively charged mRNA vaccine does not have, including higher transfection ability, strong anti-serum ability, rapid lysosome escape ability, spleen targeting, better immunotherapeutic activity and biosafety. Likewise, we also found that such a coating strategy is not applicable to the development of all mRNA nanovaccines, and the existence of cholesterol may be detrimental to the coating of liposome/mRNA complexes, which provides theoretical support for the development of mRNA liposome nanovaccines based on the coating strategy. Additionally, our research also proposed potential research directions for exploring whether other anionic polymers have similar functions and how the composition of the liposome prescription affects the preparation of nanoparticle vaccines by coating strategies. Our work may provide the initial framework to continue the development of gene vectors and explore the possibility of improving the delivery of existing gene vectors by synthesizing functionalized anions.

Acknowledgments

This study was supported by the National Key Research and Development Program of China (2021YFE0206600), the Sichuan Province Science and Technology Support Program (2021YFSY0008 and 2020YJ023, China), the Translational Medicine Fund of West China Hospital (CGZH19002, China) and the 1.3.5 Project for Disciplines of excellence, West China Hospital, Sichuan University (ZYGD18020/ZYJC18006, China).

Author contributions

Xiangron Song and Xing Duan designed the research. Xing Duan and Yi Zhang carried out the experiments and performed data analysis. Mengran Guo, Na Fan, Kepan Chen, Shugang Qin, Wen Xiao, Qian Zheng; participated part of the experiments. Hai Huang provided experimental drugs and quality control. Xing Duan and Yi Zhang wrote the manuscript. Xiangron Song and Shugang Qin revised the manuscript. All of the authors have read and approved the final manuscript.

Conflicts of interest

The authors have no conflicts of interest to declare.

Appendix A. Supporting information

Supporting data to this article can be found online at https://doi.org/10.1016/j.apsb.2022.08.015.

References

1. Pardi N, Hogan MJ, Porter FW, Weissman D. mRNA vaccines—a new era in vaccinology. *Nat Rev Drug Discov* 2018;**17**:261–79.
2. Wang Y, Zhang Z, Luo J, Han X, Wei Y, Wei X. mRNA vaccine: a potential therapeutic strategy. *Mol Cancer* 2021;**20**:33.
3. Islam MA, Rice J, Reesor E, Zope H, Tao W, Lim M, et al. Adjuvant-pulsed mRNA vaccine nanoparticle for immunoprophylactic and therapeutic tumor suppression in mice. *Biomaterials* 2021;**266**:120431.
4. Feng C, Li Y, Ferdows BE, Patel DN, Ouyang J, Tang Z, et al. Emerging vaccine nanotechnology: from defense against infection to sniping cancer. *Acta Pharm Sin B* 2022;**12**:2206–23.
5. He Q, Gao H, Tan D, Zhang H, Wang JZ. mRNA cancer vaccines: advances, trends and challenges. *Acta Pharm Sin B* 2022;**12**:2969–89.
6. Polack FP, Thomas SJ, Kitchin N, Absalon J, Gurtman A, Lockhart S, et al. Safety and efficacy of the BNT162b2 mRNA Covid-19 vaccine. *N Engl J Med* 2020;**383**:2603–15.
7. Sahin U, Muik A, Derhovanessian E, Vogler I, Kranz LM, Vormehr M, et al. COVID-19 vaccine BNT162b1 elicits human antibody and T(H)1 T cell responses. *Nature* 2020;**586**:594–9.
8. Baden LR, El Sahly HM, Essink B, Kotloff K, Frey S, Novak R, et al. Efficacy and safety of the mRNA-1273 SARS-CoV-2 vaccine. *N Engl J Med* 2021;**384**:403–16.
9. Corbett KS, Flynn B, Foulds KE, Francica JR, Boyoglu-Barnum S, Werner AP, et al. Evaluation of the mRNA-1273 vaccine against SARS-CoV-2 in nonhuman primates. *N Engl J Med* 2020;**383**:1544–55.
10. Cheng Q, Wei T, Farbiak L, Johnson LT, Dilliard SA, Siegwart DJ. Selective organ targeting (SORT) nanoparticles for tissue-specific mRNA delivery and CRISPR-Cas gene editing. *Nat Nanotechnol* 2020;**15**:313–20.
11. Guan S, Rosenecker J. Nanotechnologies in delivery of mRNA therapeutics using nonviral vector-based delivery systems. *Gene Ther* 2017;**24**:133–43.
12. Zhi D, Bai Y, Yang J, Cui S, Zhao Y, Chen H, et al. A review on cationic lipids with different linkers for gene delivery. *Adv Colloid Interface Sci* 2018;**253**:117–40.
13. Zoulikha M, Xiao Q, Boafo GF, Sallam MA, Chen Z, He W. Pulmonary delivery of siRNA against acute lung injury/acute respiratory distress syndrome. *Acta Pharm Sin B* 2022;**12**:600–20.
14. Qian Y, Liang X, Yang J, Zhao C, Nie W, Liu L, et al. Hyaluronan reduces cationic liposome-induced toxicity and enhances the anti-tumor effect of targeted gene delivery in mice. *ACS Appl Mater Interfaces* 2018;**10**:32006–16.
15. Zhang BF, Xing L, Qiao JB, Cui PF, Wang FZ, Zhang JL, et al. *In vivo* synergistic antitumor effect and safety of siRNA and lonidamine dual-loaded hierarchical targeted nanoparticles. *Int J Pharm* 2016;**506**:207–13.
16. Lv H, Zhang S, Wang B, Cui S, Yan J. Toxicity of cationic lipids and cationic polymers in gene delivery. *J Control Release* 2006;**114**:100–9.
17. Wei X, Shao B, He Z, Ye T, Luo M, Sang Y, et al. Cationic nanocarriers induce cell necrosis through impairment of Na(+)/K(+)-ATPase and cause subsequent inflammatory response. *Cell Res* 2015;**25**:237–53.
18. Zhou Z, Liu X, Zhu D, Wang Y, Zhang Z, Zhou X, et al. Nonviral cancer gene therapy: delivery cascade and vector nanoproperty integration. *Adv Drug Deliv Rev* 2017;**115**:115–54.
19. Yu M, Zheng J. Clearance pathways and tumor targeting of imaging nanoparticles. *ACS Nano* 2015;**9**:6655–74.
20. Degors IMS, Wang C, Rehman ZU, Zuhorn IS. Carriers break barriers in drug delivery: endocytosis and endosomal escape of gene delivery vectors. *Acc Chem Res* 2019;**52**:1750–60.

21. McKinlay CJ, Benner NL, Haabeth OA, Waymouth RM, Wender PA. Enhanced mRNA delivery into lymphocytes enabled by lipid-varied libraries of charge-altering releasable transporters. *Proc Natl Acad Sci U S A* 2018;**115**. E5859-e66.
22. Miao L, Zhang Y, Huang L. mRNA vaccine for cancer immunotherapy. *Mol Cancer* 2021;**20**:41.
23. Yang K, Mesquita B, Horvatovich P, Salvati A. Tuning liposome composition to modulate corona formation in human serum and cellular uptake. *Acta Biomater* 2020;**106**:314−27.
24. Guo Q, Jiang C. Delivery strategies for macromolecular drugs in cancer therapy. *Acta Pharm Sin B* 2020;**10**:979−86.
25. Zhang L, Wu S, Qin Y, Fan F, Zhang Z, Huang C, et al. Targeted codelivery of an antigen and dual agonists by hybrid nanoparticles for enhanced cancer immunotherapy. *Nano Lett* 2019;**19**: 4237−49.
26. Lu C, Stewart DJ, Lee JJ, Ji L, Ramesh R, Jayachandran G, et al. Phase I clinical trial of systemically administered TUSC2(FUS1)-nanoparticles mediating functional gene transfer in humans. *PLoS One* 2012;**7**:e34833.
27. Porteous DJ, Dorin JR, McLachlan G, Davidson-Smith H, Davidson H, Stevenson BJ, et al. Evidence for safety and efficacy of DOTAP cationic liposome mediated CFTR gene transfer to the nasal epithelium of patients with cystic fibrosis. *Gene Ther* 1997;**4**: 210−8.
28. Yan Y, Du C, Duan X, Yao X, Wan J, Jiang Z, et al. Inhibiting collagen I production and tumor cell colonization in the lung *via* miR-29a-3p loading of exosome-/liposome-based nanovesicles. *Acta Pharm Sin B* 2022;**12**:939−51.
29. Lopez-Mendez TB, Santos-Vizcaino E, Pedraz JL, Orive G, Hernandez RM. Cell microencapsulation technologies for sustained drug delivery: latest advances in efficacy and biosafety. *J Control Release* 2021;**335**:619−36.
30. Rehman A, Jafari SM, Tong Q, Riaz T, Assadpour E, Aadil RM, et al. Drug nanodelivery systems based on natural polysaccharides against different diseases. *Adv Colloid Interface Sci* 2020;**284**: 102251.
31. Toragall V, Jayapala N, Muthukumar SP, Vallikanan B. Biodegradable chitosan-sodium alginate-oleic acid nanocarrier promotes bioavailability and target delivery of lutein in rat model with no toxicity. *Food Chem* 2020;**330**:127195.
32. Chen M, Zeng Z, Qu X, Tang Y, Long Q, Feng X. Biocompatible anionic polyelectrolyte for improved liposome based gene transfection. *Int J Pharm* 2015;**490**:173−9.
33. Kowalski PS, Rudra A, Miao L, Anderson DG. Delivering the messenger: advances in technologies for therapeutic mRNA delivery. *Mol Ther* 2019;**27**:710−28.
34. Lou G, Anderluzzi G, Schmidt ST, Woods S, Gallorini S, Brazzoli M, et al. Delivery of self-amplifying mRNA vaccines by cationic lipid nanoparticles: the impact of cationic lipid selection. *J Control Release* 2020;**325**:370−9.
35. Kim H, Okamoto H, Felber AE, Polomska A, Morone N, Heuser JE, et al. Polymer-coated pH-responsive high-density lipoproteins. *J Control Release* 2016;**228**:132−40.
36. van den Berg LM, Ribeiro CM, Zijlstra-Willems EM, de Witte L, Fluitsma D, Tigchelaar W, et al. Caveolin-1 mediated uptake *via* langerin restricts HIV-1 infection in human Langerhans cells. *Retrovirology* 2014;**11**:123.
37. Hillaireau H, Couvreur P. Nanocarriers' entry into the cell: relevance to drug delivery. *Cell Mol Life Sci* 2009;**66**:2873−96.
38. Luzio JP, Pryor PR, Bright NA. Lysosomes: fusion and function. *Nat Rev Mol Cell Biol* 2007;**8**:622−32.
39. Steele TW, Shier WT. Dendrimeric alkylated polyethylenimine nanocarriers with acid-cleavable outer cationic shells mediate improved transfection efficiency without increasing toxicity. *Pharm Res* 2010; **27**:683−98.
40. Cheung CY, Murthy N, Stayton PS, Hoffman AS. A pH-sensitive polymer that enhances cationic lipid-mediated gene transfer. *Bioconjugate Chem* 2001;**12**:906−10.
41. Kranz LM, Diken M, Haas H, Kreiter S, Loquai C, Reuter KC, et al. Systemic RNA delivery to dendritic cells exploits antiviral defence for cancer immunotherapy. *Nature* 2016;**534**:396−401.
42. Pollard C, Rejman J, De Haes W, Verrier B, Van Gulck E, Naessens T, et al. Type I IFN counteracts the induction of antigen-specific immune responses by lipid-based delivery of mRNA vaccines. *Mol Ther* 2013;**21**:251−9.
43. Yin H, Kanasty RL, Eltoukhy AA, Vegas AJ, Dorkin JR, Anderson DG. Non-viral vectors for gene-based therapy. *Nat Rev Genet* 2014;**15**:541−55.
44. Wang W, Feng S, Ye Z, Gao H, Lin J, Ouyang D. Prediction of lipid nanoparticles for mRNA vaccines by the machine learning algorithm. *Acta Pharm Sin B* 2022;**12**:2950−62.